DIET-INDUCED-OBESITY SUPPRESSES BETA-CATENIN AND PROMOTES CELL PROLIFERATION DURING COLON DEVELOPMENT

BY

GUANYING XU

THESIS

Submitted in partial fulfillment of the requirements
for the degree of Master of Science in Food Science and Human Nutrition
with a concentration in Human Nutrition
in the Graduate College of the
University of Illinois at Urbana-Champaign, 2018

Urbana, Illinois

Master's Committee:

Associate Professor Yuan-Xiang Pan, Chair
Associate Professor Hong Chen
Assistant Professor Anna E. Arthur

ABSTRACT

Diet induced obesity (DIO), resulting from long-term consumption of a high fat diet, modifies multiple signaling pathways. These response pathways are closely associated with cell proliferation, inflammation and immune responses. The main goal of this present study is to investigate the impact from diet-induced obesity (DIO) on the regulation of expression of β-catenin and its localization, causing downstream impacts on cellular development, inflammation and immune system in the mouse colon.

In this study, 5-week-old male mice were fed either a control diet (CON, 10% kcal from fat) or a high-fat diet (HF, 45% kcal from fat) for 11 weeks. Body fat percentage and food intake results indicate significant difference between two groups of mice. The effects of DIO on mRNA expression of related genes in selected pathways in the colon tissue were analyzed in both control and DIO mice. *Wnt 2, Wnt5a, Wnt7b, Axin1, APC, CTNNB1* and *c-Myc* were significantly decreased while *Sfrp2* and *Sfrp 5* were significantly increased in DIO group, suggesting that Wnt signaling pathway were suppressed by DIO. The expression of *p21* and *Raf-1* were also significantly decreased in DIO group, while *Cyclin D1* was increased, suggesting that DIO has impact on cell proliferation. Immunofluorescent staining results suggested that repressed Wnt signaling prevented β-catenin translocation and its nuclear accumulation, while Ki-67 showed a stronger signal intense in DIO mice.

Overall, this study shows that DIO suppressed β-catenin expression as well as nuclear accumulation, which inhibited Wnt signaling pathway while promoted cell proliferation in the colon of DIO mouse. Furthermore, findings from current study may be applied as colon health indicator for clinical study in future.

ACKNOWLEDGEMENTS

I would like to first thank my advisors. Dr. Yuan-Xiang Pan and Dr. Hong Chen, for their assistance and support throughout the completion of my master's thesis project. This work was financially supported in part by the Campus Research Board of University of Illinois at Urbana-Champaign and the USDA Cooperative State Research, Education and Extension Service, Hatch project numbers # ILLU-698-923 and ILLU-698-379. Also, I would like to thank Adam Kriska and Paul Jung for assisting the colon sample collection, and to express my sincere gratitude to Dr. Mayandi Sivaguru, Dr. Austin Cyphersmith and Dr. Kingsley Boateng at *CARL R. WOESE Institute for Genomic Biology* for their time and for those precious advice provided in terms of colon histology. I wish to thank my committee members as well, for the support and suggestion given. Finally, I must thank my wonderful and extremely supportive family and my adorable friends, for their endless love and encouragement.

TABLE OF CONTENTS

CHAPTER 1
INTRODUCTION

Obesity and overweight, as previous research suggests, are most often caused by a lack of energy balance, which, in this case, means that the energy intake is greater than energy output. According to surveys conducted by the Centers of Disease Control and Prevention (CDC), which published by National Heart, Lung and Blood Institute (NIH) in 2012, more than 65% of adults in the U.S are considered to be overweight or obese and more than 30% of children (ages 2 to 19) are considered to be either overweight or obese. Moreover, each year in the United States, obesity is involved in 400,000 deaths and costs $117 billion in health-care and related expenses (1). These statistics have no doubt raised obesity to one of the biggest public health concerns and challenges in this country, especially considering the associated risks of chronic diseases, including cancer development, linked with obesity. Diet-induced-obesity (DIO), as one of the most commonly studied topics among obesity related cases in animal experiments, has been tightly linked to several molecular and physiological dysfunctions including leptin resistance, glucose intolerance, oxidative stress promotion, ovarian morphology and eccentric hypertrophy (2-5). The mechanism behind these changes involves several important signaling pathways that have been discovered in human and animal models, including the upregulated inflammatory signaling pathway (inflammatory c-Jun N-terminal kinase and NF-kappa B signaling pathway), disrupted leptin signaling pathway, induced estrogen signaling (ER-independent E2-ERa) pathway, inhibited mTOR signaling pathway, impaired or inhibited AMPK and SREBP signaling pathway, and WNT signaling pathway (6-11).

The Wingless/Integrase 1 (Wnt) signaling pathway, which is proved to be highly conserved in multicellular eukaryotic animals, plays an essential role in embryonic development and tissue homeostasis by regulating cellular processes such as proliferation apoptosis,

differentiation, polarization and motility (12-14). Furthermore, Wnt signaling is able to modulate various immune cell functions, including cytokine production, immune cell migration or differentiation, consequently shape inflammation and infection process and host response to pathogens (15-17). Three Wnt signaling cascades are included in Wnt signaling pathway: the Wnt/β-catenin pathway (canonical), the β-catenin independent Wnt/Ca^{2+} pathway, and Wnt/Planar cell polarity pathway (both non-canonical) (18). In canonical pathway, signals mostly go through GSK3β, Axin1, APC or other set of cytoplasmic components to reach β-catenin and form a complex with TCF/LEF in the nucleus (19). This complex then triggers the expression of downstream target genes including *c-Myc*, *VEGF* and *Cyclin D1,* which regulates cell proliferation and angiogenesis (20-22). Non-canonical Wnt, on the other hand, can also regulate angiogenesis by targeting VEGE receptor Flt1 (also knowns as VEGFR1) (23), and cell-proliferation, by binding to its receptor Ryk with Wnt5a (24, 25). Interestingly, many studies demonstrated that Wnt/β-catenin pathway is a very important indicator during colorectal cancer (CRC) development, based on following reasons: a. muted Wnt/β-catenin pathway was detected in approximately 90% of CRC cases (26); b. Wnt/β-catenin signaling is proved to be essential for aberrant expansion of cancer stem/tumor-initiating cells (27); c. Wnt/β-catenin signaling can induce the expression of epithelial mesenchymal transition (EMT) transcription factors, which contributes to the metastasis of CRC (28).

Notably, β-catenin from canonical Wnt signaling pathway plays a critical role in promoting proliferation and differentiation of stem cells in the intestinal crypts of epithelium. However, the mechanisms behind these regulations are not fully understood (29).

The purpose of this present study is to investigate the role of DIO on the regulation of β-catenin expression and its impacts on other signaling pathways, which results in downstream

protein expression changes and differential responses triggered in epithelial cell development in the colon. We hypothesized that DIO would suppress β-catenin expression, which leads to a downregulation of Wnt pathway target genes, such as *c-Myc*, and differential regulation of colon cell proliferation.

CHAPTER 2
LITERATURE REVIEW

High-Fat Diet (HFD) and Diet-Induced-Obesity (DIO) have been proved to play a significant role in regulating Wnt signaling pathway in several organs (or tissues) in animal model.

SKELETAL DEVELOPMENT

Research indicates that HFD and its consequence, DIO, can suppress Wnt/β-catenin in the bone of animal models. One study focusing on effects of high-fat diet on bone with male mice model has suggested that Non-Esterified Fatty Acids (NEFA) treatment depressed β-catenin expression and activity *in vitro*, without causing effect on Wnt inhibitors such as DKK1, and it concluded that high fat diet can inhibit Wnt signaling and lead to less bone mass (30). Same discovery was claimed in one other study focusing on bone marrow adiposity and stromal cell differentiation. This study discovered that Wnt/β-catenin expression was significantly downregulated by HFD in bone of growing male rats (31). A more recent study focusing on bone acquisition in young male mice also concludes that DIO suppressed Wnt/β-catenin signaling can lead to less bone mass in male mice based on their observations (32). In Lu's study, comparing to control group, gene expression of the key canonical Wnt signaling molecule, β-catenin, was found significantly downregulated in tibia bone collected from 8-week HFD treated male mice, confirmed by qPCR and western blot. To understand the mechanism through which Wnt/β-catenin regulates bone formation and osteoblast function, Dr. Frey and her team conducted a study using C57BL/6 Lrp5 knockout and Lrp6 knockout male mice as animal model. In this study, Lrp5 was confirmed to be the coreceptor that stabilizes β-catenin in Wnt signaling pathway. With Lrp5 knockout, there were reduced osteoblasts and osteocytes exhibited in

postnatal bone mass, while body fat, including triglyceride and free fatty acids levels, increased in animal model. Therefore, the mechanism through which Wnt/β-catenin alters bone mass and body composition proposed by the author is: Wnt/β-catenin signaling regulates bone formation and fatty acid metabolism in animal model by binding with coreceptor Lrp5, rather than Lrp6, which further reallocates fuel sources and alters body composition (33).

ADIPOGENESIS PROGRAMMING

HFD and DIO were also observed to suppress Wnt/β-catenin signaling pathway in adipose tissue of animal model. One study suggests that the expression of several genes involved in canonical Wnt signaling pathway (Wnt1 and Wnt3a) was downregulated with HFD treatment after 63 days in subcutaneous adipose tissues in rats, as well as the Wnt ligands Wnt1, Wnt3a and Wnt10b, which were all downregulated in both subcutaneous and epididymal adipose tissue (AT) significantly ($P < 0.05$) at 63 d of experiment. Furthermore, it found that canonical Wnt receptors such as Fzd1, Fzd2 and Fzd5 was all lowered significantly ($P < 0.05$) in AT with initiation of HFD at 63 d. Wnt signaling intermediates, GSK3β and β-catenin, was also found lower in epididymal adipose tissue with HFD at 63d, while no difference in expression was observed in subcutaneous AT (34). Consistent with their observations, a recent published study also found that early stage of obesity model significantly downregulates β-catenin mRNA expression ($P < 0.05$). This study also performed western blot to confirm the change of β-catenin expression on protein level, which was also decreased with obesity model, in the adipose tissue of male Sprague-Dawley rats. Furthermore, this study discovered that the expression of canonical Wnt signaling players (Wnt3a) was also downregulated in obese rat model, while wnt5a, a member of non-canonical Wnt signaling pathway, was significantly upregulated.

Together, the author summarized that early stage of obesity may affect cell proliferation and regulate adipogenesis through Wnt/β-catenin signaling pathway as well as non-canonical Wnt signaling, limiting the hyperplasia of adipocytes in animal model (35). A potential mechanism through which Wnt/β-catenin regulates adipogenesis programming, discovered by Dr. Chen in 2015, is through the regulation of its effector transcription factor 7-like-2 (TCF7L2). TCF7L2 is a component in Wnt signaling pathway and is commonly connected with diabetes and other metabolic disorders. In HFD fed mice, epidydimal fat TCF7L2 mRNA level was found lower than control diet fed mice, which is corresponding to the downregulated Wnt/β-catenin signaling pathway (36). Although the role TCF7L2 plays in adipocytes development remains unknow as recently published study points out, it is clear that TCF7L2 is crucial for maintaining the normal function of adipocytes and regulating adipogenesis, while downregulation of TCF7L2 could result in severe consequences such as impaired glucose tolerance and increased adipocyte insulin resistance (37).

HEPATIC FUNCTION

HFD and DIO have been proved to affect hepatic function significantly by regulating multiple signaling pathways, including both canonical and non-canonical Wnt signaling pathways, and may contribute to the development of certain diseases such as liver steatosis and fibrosis, even cancer. To investigate the roles of Wnt/β-catenin signaling pathway in regulating hepatic fat accumulation, one study measured β-catenin protein level in the liver of obese rats and found that obesity significantly downregulates β-catenin protein level compared to lean group, indicating an inhibited canonical Wnt signaling pathway in liver. This consequently leads to an overall increase in hepatic fat and affect liver functions, increasing risk of steatohepatitis

and further hepatocarcinogenesis (38). Another study, aiming to clarify the role of β-catenin in mouse liver fibrosis, found that hepatic β-catenin regulates systemic energy homeostasis through hepatic fatty acid oxidation, ketogenesis and mitochondrial functions, and therefore affects the development of DIO. The author concluded that β-catenin may be the key player in the pathogenesis of fatty liver disease, DIO and insulin resistance (39). Besides canonical Wnt signaling pathway, β-catenin is also found to interact with other signaling pathway to affect liver function. In Zhai's study, β-catenin reduces mRNA expression and activity level of sterol regulatory element-binding protein-1c (SREBP-1c) in mouse liver, which can inhibit hepatic stellate cells (HSCs) activation, a key step in hepatic fibrogenesis. Because SREBP-1c expression plays important role in leptin regulation, and leptin induced liver fibrosis in mice, the author believe that this is a potential mechanism for β-catenin to contribute to liver fibrogenesis (40). In conclusion, because of the complexity of Wnt/β-catenin signaling in liver, the mechanism through which this pathway regulate hepatic function and disease development remains unclear based on current literature, however, it is evident that Wnt/β-catenin signaling is downregulated by DIO in liver and this downregulation is connected with various DIO related liver diseases including insulin resistance, leptin regulation, liver fibrosis and hepatocarcinogenesis.

ENERGY METABOLISM AND GLUCOSE HOMEOSTASIS

Besides glucose intolerance and insulin resistance altered by Wnt/β-catenin in adipocytes and liver, recent work also highlights that Wnt signaling plays critical role in the neuroendocrine control of glucose and energy metabolism. In a research conducted using C57BL/6JRj male mice, a significantly downregulated expression of the ligands Wnt7a ($P = 0.004$) and Wnt4

(P=0.038) was found in the hypothalamic arcuate nucleus (ARC) of leptin-deficient obese mice, in comparison with the expression in control wild type mice. The mRNA expression of Wnt signaling downstream target genes Axin-2 (P=0.002) and CyclinD1 (P=0.043) in the hypothalamic arcuate nucleus (ARC) of leptin-deficient obese mice was also found downregulated significantly. The observations support the conclusion that hypothalamic Wnt signaling is impaired during obesity, which is crucial for high-fat diet-induced weight gain as well as glucose homeostasis (41).

Wnt/β-catenin signaling was also found to be associated with susceptibility to type 2 diabetes by altering β-cell proliferation and total mass in the pancreas. In Dr. Elghazi's study published in 2012, the author observed that with β-catenin deletion, mature β-cell proliferation and mass were impaired in adult male mice, which alters glucose homeostasis in the animal model. Besides, abnormal insulin sensitivity was also discovered after depletion of β-catenin, which might be caused by the increased motor activity in the basal state of mice. Although how Wnt/β-catenin signaling pathway alters different tissue to control glucose and insulin sensitivity is not completely understood yet as the author suggests, it is clear that this signaling pathway play important role in pancreas, especially for insulin secretion and function, and this could be another mechanism HFD/DIO affect glucose homeostasis in animal model (42).

KIDNEY FUNCTION

Although the studies mentioned above all observed down-regulated Wnt signaling pathway in different organs using animal models, either canonical or non-canonical, during high-fat-diet treatment or by obesity, HFD/DIO was also found to upregulate Wnt/β-catenin in

specific tissue. For example, one study conducted using male C57/BJ mice found that mRNA expression of genes involved in Wnt signaling, Wnt1 and Wnt16, were upregulated in the kidney of HFD mice group comparing the control group. Despite the fact that the mechanism behind this observation remains unclear and it requires further investigation to be fully established, this study indicates that HFD regulated Wnt signaling pathway can be further linked to lipid transport and metabolism related to kidney function (43).

EARLY LIFE PROGRAMMING

Few studies have done focusing on HFD-mediated β-catenin expression in placenta of animal model. In Dr. Strakovsky's study published in 2012, Wnt/β-catenin signaling inhibitor Dickkopf homolog 1 (Xenopus laevis) (DKK1) mRNA expression was found significantly lowered in placentas of obesity prone (OP) rats fed with HFD. Meanwhile, nuclear β-catenin protein expression was significantly increased in OP rat placentas comparing to obesity resistance (OR) rats. Therefore, the author concluded that Wnt/β-catenin signaling pathway is dysregulated in the placenta of obese rats and is directly involved in placental lipid metabolism: Aberrant Wnt/β-catenin with decreased DKK1 expression leads to less decidual/junctional thickness of placenta and consequently decreased placental efficiency (44). The author also proposed that this activation of Wnt/β-catenin signaling may trigger the expression of Ppard, a potent inducer of adipogenesis and lipogenesis, which could serve as a signal between mother and fetus and further affect fetus early life programming.

COLON HEALTH

Previous studies suggest that DIO is tightly connected to colon carcinogenesis. As a prospective cohort study has reported, obesity, caused by high energy and high fat intake, was associated with increased risk of colon cancer development as well as increased death rate (45, 46). A recently published review article utilizing next generation RNA sequencing concluded that DIO (caused by HFD) stimulates multiple pathways involved in inflammation (i.e. IL-6, IL-8 and dendritic cell and leukocyte signaling**)** and tumorigenesis in mouse colon (i.e. eNOS signaling and VEGF signaling), which are similar to those found in human colon cancer with inflammatory microsatellite instability (47). Wnt/β-catenin signaling pathway, among all the pathways altered by DIO in colon, is generally believed to be elevated after long-term consumption of high fat diet in animal model, while the mutation of transcription factor β-catenin is commonly believed to be a key player in the development of CRC. In a recent published study, upregulation of β-catenin gene and protein expression were detected in colon epithelium in male Wistar rats fed HFD for 17 weeks. This study failed to illustrate the detailed mechanisms through which HFD regulate β-catenin expression, and to demonstrate any downstream regulation involved in CRC development that is caused by the change of β-catenin expression directly. However, the authors concluded that HFD-mediated tumorigenesis in colon is associated with increased cell cycle progression as well as the inflammation responses triggered by the upregulation of β-catenin. Furthermore, this study suggests that HFD not only increases β-catenin expression, but also NF-κB, another transcription factor that is responsible for inflammation responses and regulation of cyclin D1 and COX-2 expression (48). On the other hand, an earlier published study proposed another mechanism, through which β-catenin regulates NF-κB expression in opposite direction: in this study, β-catenin was found to

physically complex with NF-κB, which reduces NF-κB DNA binding capability, therefore decreased its transactivation activity and ultimately its target gene expression. The author concluded that β-catenin can inhibit NF-κB activity and repress the expression of Fas, a NF-κB target gene. Fas is a cell surface receptor in tumor necrosis factor receptor (TNFR) family, it is expressed in normal epithelial cells to mediate apoptosis and is usually downregulated in colon carcinomas. Because β-catenin is an inhibitor of NF-κB, while Fas-induced apoptosis requires NF-κB, the activation of β-catenin therefore contributes to the oncogenesis in both human colon and human breast cancer cell lines (49).

In summary, DIO from HFD was observed in several cases to activate Wnt/β-catenin signaling pathway in colon, which further triggers inflammation responses through other signaling pathways such as NF-κB and regulate colon epithelial cell proliferation as well. Aberrant Wnt/ β-catenin activity in colon therefore is considered as a biomarker for colon carcinogenesis. However, most of these studies are done using azoxymethane treated animal model rather than healthy animals, thus it remains unclear how DIO alters Wnt/β-catenin signaling pathway in heathy animal model.

CHAPTER 3
METHODOLOGY

ANIMAL AND DIETS

Male CBA mice (The Jackson Laboratory) were purchased at 4 weeks of age and were accommodated in standard polycarbonate cages (4 mice per cage) at a humidity-and temperature-controlled room at Edward R. Madigan Laboratory for one week prior to experiment in order to acclimatize. At 5 weeks of age, male mice were divided into control diet (CON; n=12) or higher-energy-density diet (DIO; n=14). Both groups were provided food and water *ad libitum* and maintained at a 12-hour light condition. Following 11 weeks of the dietary intervention, mice in each diet group were sacrificed by CO_2 asphyxiation, colon tissue samples from each mouse were collected. All procedures were approved by the Institutional Animal Care and Use Committee at the University of Illinois at Urbana-Champaign.

Mice in the DIO group were provided a high energy dense diet containing 4.73 kCal/g, consisting of 20% (kCal%) protein, 35% carbohydrates and 45% fat (D12451i, Research Diet Inc.), for 10 weeks to induce obesity (DIO). Meanwhile, mice treated with control diet were provided a diet containing 3.85 kCal/g, consisting of 20% (kCal%) protein, 70% carbohydrates and 10% fat (D12450Hi, Research Diet Inc.) for 10 weeks. The formula of higher-energy-density diet was modified using lard as the major source of energy, while control diet used corn starch. (**Supplementary Table 1**).

CBA mouse strain is often used in research fields such as immunology, oncology and pharmacology. The CBA has life-span going from 69 up to 117 weeks, depending on sex. Previous study used CBA mouse to investigate the effects of thalidomide on colorectal cancer liver metastases (50). Besides, the male CBA is recommended (The Jackson Laboratory) to be

applied for diabetes and obesity research, particularly, for obesity-induced insulin resistance (51), maturity-onset diabetes-obesity syndrome (52) and hearing loss resulting from high-fat-diet-induced type 2 diabetes (53). Because CBA has been proved to be susceptible to diet-induced-obesity and shows steady growth rate with high fat diet, it is selected to conduct the current study.

Food intake data of every cage was recorded weekly during experiment period, while magnetic resonance imaging (MRI) was conducted monthly. Behavioral changes and stress responses, such as hair loss, were monitored daily.

COLON TISSUE SAMPLING

After 10 weeks of feeding, mice from both diet groups with sedentary treatment were randomly selected and killed by CO_2 asphyxiation. The entire colon was immediately and carefully removed and divided to proximal and distal half equally, by measuring the length from cecal junction to rectal junction. Both proximal and distal colon sampled were immediately dipped in cold (cooled by liquid nitrogen) 2-methylbutane (Thermo Fisher Scientific, Waltham, MA) until completely frozen, then stored using aluminum foil labeled on it in -80 °C freezer for further experiments and histological analysis.

QUANTITATIVE RT-PCR

Scraped proximal colon tissues (40-50 mg per animal) were grounded using liquid nitrogen and treated with TRIzol Reagent (Thermo Fisher Scientific, Waltham, MA). Total RNA

was isolated according to the manufacturer's instructions (ZYMO RESEARCH CORP.) using Direct-zol RNA MiniPrep Plus Kit (ZYMO RESEARCH CORP). RNA concentrations were measured by a Spectrophotometer (NanoDrop 2000, Thermo Fisher Scientific, Waltham, MA). cDNA was synthesized from RNA using the High Capacity cDNA Reverse Transcription Kit (Applied Biosystems, Foster City, CA) in a Thermal Cycler 2720 (Applied Biosystems). In each reaction system, 1000 ng (with concentration of 100 ng/μL) of total RNA were added in 10 μL mixture containing 2 μL 10× RT buffer, 0.8μL 100mM dNTPs, 2 μL 10× RT random primers, 1 μL 50U/μL MultiScribe Reverse Transcriptase and 4.2 μL Nuclease-free H_2O. cDNA synthesis was performed using the following program: 25 °C for 10 minutes, 37 °C for 2 hours, and 85 °C for 5 seconds. Synthesized cDNA was then analyzed by PCR in StepOnePlus Real-time q-PCR system (Applied Biosystems). In each reaction, 5 ng of synthesized cDNA was used in a 10 μL volume containing 5 μL of Quanta PerfecTa SyBR Green FastMix ROX (2x, Quantabio), 0.4 μL of foward primer (5 μM), 0.4 μL of reverse primer (5 μM) and 2.2 μL Nuclease-free H_2O. q-PCR was performed using the following program: 95 °C for 10 minutes, followed by 45-50 cycles of 95 °C for 15 seconds and 60 °C for 1 minute. After q-PCR, melting curves were acquired stepwise from 55 to 95 °C to ensure that a single product was amplified in the reaction.

Reference genes *L7a*, *GAPDH* and *β-Actin* were used as internal controls for result normalization. Gene expression quantity gained during q-PCR was analyzed and generated by StepOne Software v2.3 (Applied Biosystems). The primers used in this study are listed in the **Supplementary Table 2.**

HISTOLOGICAL ANALYSIS

Unfixed, frozen colon samples were embedded in Tissue-Tek OCT compound (VWR, Radnor, PA) prior to sectioning and cut to 14 μm thickness using a Leica CM3050 S cryostat (Leica Microsystems, Inc., IL) -20 °C. After sectioning, OCT was removed from sections by washing with 1X PBS and double distilled water, sections were then fixed in 70% ethanol and stained with hematoxylin (Thermo Fisher Scientific, Waltham, MA) and eosin (Thermo Fisher Scientific, Waltham, MA)) for histological analysis. Slides were scanned using Nanozoomer Digital Pathology system with magnification of 20X (Hamamatsu Photonics, K.K., Japan), 6 animals from each group, three 350 μm x 350 μm blocks from each animal were randomly selected to do image analysis. Image analysis was performed by Image J software (Rasband, W.S., ImageJ, U. S. National Institutes of Health, Bethesda, Maryland, USA, http://imagej.nih.gov/ij/, 1997-2017).

IMMUNOFLUORESCENT STAINING

Slides with unfixed, frozen colon were embedded in Tissue-Tek OCT compound (VWR, Radnor, PA) and cut to 14 μm thickness sections using Leica CM3050 S cryostat (Leica Microsystems, Inc., IL) at -20 °C, sections were stored in -80 °C before immunofluorescence. When conduct immunofluorescent staining, slides were first washed in 1X PBS and fixed in 4% formaldehyde. Then, slides were blocked with blocking buffer (1X PBS/5% normal goat serum/0.05% Triton X-100) and incubated with 1) primary antibody β-Catenin (D10A8) XP® Rabbit mAb (1:100 dilution, Cell Signaling Technology, Danvers, MA) at 4 °C overnight. After primary incubation, slides were washed again with 1X PBS and then incubated with Anti-rabbit

IgG (H+L), F(ab')2 Fragment (Alexa Fluor® 488 Conjugate) secondary antibody (1:100 dilution, Cell Signaling Technology, Danvers, MA) at room temperature for one hour; 2) primary antibody Alexa Fluor® 488 anti-mouse/human Ki-67 (1:100 dilution, BioLegend, San Diego, CA). After primary and secondary incubation, all slides were rinsed in 1X PBS again and incubated with DyLight 554 Phallioidin (1:50 dilution, Cell Signaling Technology, Danvers, MA) and DRAQ5 (1:100 dilution, Cell Signaling Technology, Danvers, MA) for 15 minutes in dark at room temperature. After incubation, slides were washed with 1X PBS, mounted with Prolong-Gold Antifade Reagent (Molecular Probes by Life Technologies, Carlsbad, CA) and dried in dark overnight at 4 °C. Pictures were taken using the Confocal LSM 700 microscope (Carl Zeiss Microscopy, LLC, United States) with magnification of 20X and 63X Oil for slides stained with β-Catenin, and LSM 880 microscope (Carl Zeiss Microscopy, LLC, United States) with 20X magnification for slides stained with Ki-67. Pictures were acquired using Zen software (Carl Zeiss AG, Ontario, CA).

β-CATENIN LOCOLIZATION AND QUANTIFICATION

The localization and quantification of β-catenin were determined using pictures gained from immunofluorescent staining. To determine the nucleus β-catenin accumulation in colon cells, data were obtained using 22 randomly selected colon cells at same location (top part of crypt where interfacing lumen) in one animal from each group. Imaris Software (Bitplane AG, Zurich, Switzerland) was applied to separate the nucleus by surface and measure the signal intensity of stained nucleus β-catenin protein within each nucleus. Final results are presented as the mean signal intensity ratio to nucleus volume (μm^3) ± SEM.

KI-67 LOCALIZATION AND QUANTIFICATION

The localization and quantification of Ki-67 were determined using pictures gained from immunofluorescent staining. To quantify Ki-67 signal intensity in colon cells, five 50 µm x 50 µm areas were selected from one captured picture in one animal from each group. ImageJ Software (NIH, Bethesda, MD) was applied to separate the nucleus and Ki-67 signal by channel and to measure the signal area of stained Ki-67 and nucleus. Final results are presented as the mean Ki-67 signal area ratio (μm^2) to nucleus signal area (μm^2) ± STD.

STATISTICAL ANALYSIS

Differences in body weight and food intake between groups were analyzed using repeated-measures one-way ANOVA and Tukey HSD test (RStudio, Version 1.0.136, Library "stats", Inc., Boston, MA). Results were reported as means ± SEM. Differences between two animal groups were considered significant at $P<0.05$.

Results from MRI data, quantitative real-time PCR analysis and immunofluorescence quantification analysis were analyzed using two-tailed t-test ((Data Analysis, Microsoft Office Excel 2016). Results were reported as means ± SEM. Differences between two diet groups were considered significant at $P<0.05$.

CHAPTER 4
RESULTS

11-WEEK OF HIGHER ENERGY DENSITY DIET INDUCED SIGNIFICANT CHANGES ON BODY WEIGHT AND BODY FAT COMPOSITION OF MICE AND SUCCESSFULLY CAUSED DIO

All mice survived the full treatment period, no mice were observed to have behavioral changes or stress responses. There was no significant difference in body weight ($P = 0.24$) and body fat percentage ($P = 0.76$) when the animal trial was started (data was measured at the first week of experiment). There was significant difference in body weight between the DIO and CON groups during the trial ($P<0.0001$, **Figure 1A**) and in average daily energy intake (kCal) per mouse throughout the trial (CON, 11.73±0.25 kCal/mouse/day; DIO, 13.78±0.27 kCal/mouse/day; $P = 0.0002$, **Figure 1B**). Significant difference in fat mass ($P<0.0001$) and body fat percentage ($P<0.0001$) between the two dietary groups was also observed, according to the MRI data collected at week 5 and week 9 (**Figure 1C**).

At the end of the treatment period, the body fat percentage (%) observed in mice fed higher-energy-density diet was 34.84 ± 0.96 compared to 25.33 ± 0.84 in control group, which is considered high enough to define the mice fed with higher-energy-density diet as “diet-induced-obesity” and matches the “fat-tissue-percent” data provided by The Jackson Laboratory for its DIO mouse model.

HISTOLOGY ANALYSIS SUGGESTS NO SIGNIFICANT DIFFERENCE ON HISTOLOGICAL STRUCTURE BETWEEN DIO MICE AND CONTROL MICE

Examined by hematoxylin and eosin (H&E) staining (n=6 in each group, three 350 μm x 350 μm image block in each animal), no significant difference was observed in the aspect of

histological structures, particularly, the average length of the crypt was not affected by DIO. **(Figure 2).**

DIO SUPPRESSED MRNA EXPRESSION OF GENES INVOLVED IN BOTH CANONICAL AND NON-CANONICAL WNT SIGNALING PATHWAY

To investigate the possible mechanism through which diet-induced-obesity regulates Wnt signaling pathway, the expression of genes/proteins involved in Wnt signaling were tested by RT-PCR of the colon sections from both groups of mice. In general, higher-energy-density diet and consequently diet-induced obesity affected the expression of *Wnt5a* in non-canonical Wnt pathway, *Wnt7b, Wnt2, Axin1, APC, Sfrp2* and *Sfrp5* in canonical Wnt pathway. Particularly, DIO also affected the mRNA expression of *CTNNB1*, which codes β-catenin, the most important player in Wnt signaling, and *c-Myc*, the downstream target genes of Wnt signaling. Notably, DIO downregulated the mRNA expression levels of *Wnt2*, *Wnt5a* ($p < 0.05$), *Wnt7b* ($p < 0.05$), *CTNNB1* ($p < 0.05$), *Axin1* ($p < 0.05$), *APC and c-Myc* ($p < 0.05$) while upregulated expression levels of *Sfrp2* ($p < 0.05$) and *Sfrp5* ($p < 0.05$) (**Table 1**).

GENES REGULATING CELL CYCLE REGULATED BY WNT SIGNALING EXPRESSED DIFFERENTLY BETWEEN TWO DIET GROUPS

As previously mentioned, Wnt signaling plays significant role in cell development and is able to mediate inflammation and immune responses by targeting or binding to different receptors. Therefore, it is reasonable to assume that the mRNA expression of genes related to these processes could be affected by suppressed Wnt signaling due to diet-induced obesity. To examine this assumption, mRNA expressions of selected genes were tested by RT-qPCR of the

colon sections from both groups of mice. These following genes mRNA expression was found to be different between control and DIO mice: *p21, Raf-1, CyclinD1*. Notably, DIO significantly downregulated the mRNA expression levels of *p21* ($p < 0.05$), *Raf-1* ($p < 0.05$), while significantly upregulated expression levels of *CyclinD1* (**Table 1**).

DIO LOWERED GENERAL ACCUMULATION OF β-CATENIN AND INDUCED DIFFERENT EXPRESSION LEVEL OF β-CATENIN ALONG THE COLONIC CRYPT

The regulation of Wnt/β-catenin signaling was examined by conducting immunofluorescent staining using β-catenin antibody). Specifically, a change of localization of β-catenin accumulation was observed during the analysis of immunofluorescent pictures between DIO mice and control group. Along the distal colonic crypt, with a magnification of 20X (**Figure 3 A-H**), we discovered that mice in DIO group have, in general, a decreased accumulation of β-catenin in the epithelia, when comparing to the control group. This decrease is more profound at the simple columnar epithelium (the top of the crypt near lumen) where most cells are absorptive columnar cells, and at the submucosa tissue. Within the colon of the DIO mice there is a visibly higher β-catenin accumulation at the bottom part of crypt near the submucosa, where stem and progenitor cells are housed. Furthermore, with a magnification of 63X Oil (**Figure 3 I-P**), a significant diet effect on the nuclear accumulation of β-catenin protein between DIO mice and mice in the control group was found, which is consistent with the mRNA expression result: DIO mice have a lower nuclear accumulation of β-catenin protein comparing to control group (**Figure 3 Q**).

DIO INDUCED HIGHER EXPRESSION OF CELL PROLIFERATION MARKER KI-67 IN COLON OF MICE

To further investigate the effect of downregulated β-catenin expression on cell proliferation in colon of mouse, immunofluorescent staining using Ki-67 antibody was performed. With a magnification of 20X, a significant diet effect on the signal intensity of Ki-67 protein between DIO mice and CON mice was observed (**Figure 4 A-H**): DIO mice have a significantly higher Ki-67 protein expression level (presented as Ki-67 signal area ratio to nucleus area) comparing to control group (**Figure 4 I)**. This result suggests that DIO mice have a higher proliferative activity level comparing to CON mice, which indicating that DIO has promoted cell proliferation in colon tissue of male mice.

CHAPTER 5
DISCUSSION

The current study utilized DIO in CBA mice to demonstrate that DIO downregulated the expression of genes involved in Wnt signaling pathway and the downstream target genes in colon. This suppression of Wnt signaling was confirmed by immunofluorescent staining, which showed that the accumulation of β-catenin protein along colon crypts was lowered in DIO mice comparing to the control mice.

DIO SUPPRESSES WNT SIGNALING EXPRESSION IN SEVERAL ORGANS

The current study suggests that DIO suppressed the Wnt signaling pathway in the distal colon of male mice. Despite the direct influence from DIO on mRNA expression of Wnt ligands such as *Wnt2*, *Wnt5a* and *Wnt7b*, in this current study we also found significant upregulations of *Sfrp2* and *Sfrp5* mRNA expression in colon of mice induced by DIO. In general, both *Sfrp2* and *Sfrp5* are linked tightly with Wnt signaling pathway function mostly as antagonist (54-59). Nevertheless, *Sfrp5* is also proved to be an anti-inflammatory adipokine that modulates metabolic dysfunction in obesity (60). However, the role *Sfrp2* plays in Wnt signaling is somehow controversial: one study found that *Sfrp2* serves as a Wnt agonist in lung cancer cells (61), however, another study claiming that it is the silencing of *Sfrp2* induces Wnt signaling in cervical cancer cell lines (62). Based on the results obtained in this current study and what has been concluded in previous study (63), it is reasonable to assume that *Sfrp2* and *Sfrp5* serve as Wnt signaling antagonists in distal colon of mice, and the aberrant expression of these genes contributes to the inhibition of Wnt signaling, which further influence lipid metabolism and facilitate adipocyte growth during DIO development.

DIFFERENTIAL LOCALIZATION OF β-CATENIN PLAYS SIGNIFICANT ROLE IN PROGNOSIS OF COLORECTAL CARCINOGENESIS

This current study has two unique discoveries regarding β-catenin localization: 1) Compared to control mice, DIO mice had less β-catenin protein expression on their muscularis mucosae and submucosa layers; 2) Compared to control mice, DIO mice had less nucleus β-catenin accumulation along the crypt. Furthermore, DIO mice express β-catenin more on the bottom of the crypt (close to submucosa layer), while control mice express β-catenin more on the top of crypt (close to lumen).

Previous research has established a significant correlation between β-catenin translocation and colorectal carcinogenesis and a potential correlation between β-catenin translocation and lymph node metastasis, colorectal cancer patient survival and colorectal cancer prognosis, indicating that the localization of β-catenin could be a crucial indicator for colorectal cancer (64-72). Particularly, one study discovered that in most colorectal tumor samples, increased β-catenin protein level were found in the cytosol and/or membrane compartment comparing to nucleus (73), which is similar to what was observed in DIO mice in this current study.

However, most studies discussed the change of β-catenin protein expression on subcellular level, especially within nucleus, without mentioning changes happened on membranous and cytosol accumulation of β-catenin, or changes of β-catenin protein expression level along colonic crypt. Furthermore, most of the findings were established based on colorectal cancer model rather than DIO model. Therefore, the findings brought up by this current study are unique and important to justify the clinical significance of investigation on DIO-triggered, different spatial localization of β-catenin in colon. Considering the link between Wnt signaling

and colorectal cancer, a potential application of this information would be, to use the spatial localization of β-catenin as an indicator to detect the abnormality of colon during early stage of carcinogenesis, rather than the protein expression. However, to establish a complete conclusion on this topic, a fully investigation using a 3D model is required for further research.

Additionally, the connection among DIO, β-catenin and Ki-67 expression remains unclear at this point, however, it is demonstrated by previous studies that the expression level of Ki-67 is correlated to the expression of *Cyclin D1*, and they may be used together as a marker for carcinogenesis and active cell proliferation(74-78). In our current study, we observed both increased Ki-67 protein expression and *Cyclin D1* mRNA expression in DIO mice, which is consistent with previous studies and further confirmed a higher proliferative activity is promoted by DIO in colon cells.

MECHANISMS THROUGH WHICH SUPPRESSED β-CATENIN REGULATES CELL CYCLE

In this current study, the mRNA expression of several genes that play significant role in cell cycle were selected and examined, among which *c-Myc*, *Raf-1*, *Axin1* and *p21* were found significantly downregulated in DIO mice while *CyclinD1* was upregulated.

The downregulation of *c-Myc* is expected, as *c-Myc* is the target gene in Wnt pathway, and DIO suppresses Wnt signaling. *c-Myc* has been reported to play crucial role in cell proliferation and differentiation through the following mechanisms: *c-Myc* revokes the transcription of cell cycle checkpoint genes such as *GADD45* and *GADD153*; inhibits the function of cyclin-dependent kinase (CDK) inhibitors; activates *Cyclin D1*, *Cyclin D2*, *Cyclin E1* and *Cyclin A2* therefore promotes cell cycle progression (79). Hence, the downregulation of *c-*

Myc caused by suppressed Wnt signaling from DIO will lead to less expression of CDK subunits and elevated expression of CDK inhibitors (80), which consequently overcomes cell-cycle arrests and causes cells to withdraw from the G1 phase.

On the other hand, previous study implied that activated Wnt/β-catenin signaling promotes expression of p21 in mesenchymal stem cells (MSCs) to regulate cellular development (81). Here, we confirmed that with a suppressed Wnt/β-catenin signaling from DIO, the expression of p21 decreased, and this decrease is likely to cause increased G2 phase arrest in cell cycle and therefore increase apoptosis (82). Additionally, a downregulated of *Raf-1* was detected in the current study in DIO mice. *Raf-1*, in general, is believed to play as pro-survival antiapoptotic factors in cell cycle (83). *Raf-1* is linked to β-catenin in breast tumorigenesis, together they are responsible for the expansion of tumor (84). However, no evidence was found to demonstrate the interaction between *Raf-1* and β-catenin in colon. One potential mechanism linking them together is through extracellular signal-regulated kinase (ERK) pathway in colon, because literature evidence suggests that β-catenin as well as *Axin1* and *APC* are involved in the activation of Ras-ERK pathway, which controls *Raf-1* expression (85, 86). Further research is necessary in order to fully investigate the connection between these pathways.

Cyclin D1 is a well-established target gene of Wnt signaling (87, 88), and controversially was observed upregulated in DIO mice. The potential explanation here could be that the decreased expression of *p21*, a main CDK inhibitor, caused a positive influence on expression of *CyclinD1* through *p53*-dependent pathway (89), which is stronger to overcome the negative influence brought by suppressed Wnt signaling. Furthermore, DIO was previously found to induce tumor growth by upregulating protein expression level of *CyclinD1* (90). Another research done in 2012 also suggests that DIO animal showed a higher protein level expression of

CyclinD1 in colon, which then be concluded as a possible mechanism through which DIO facilitate colon tumor formation (91).

CONCLUSION

In this current study, we proposed a schematic presented in ***Figure 5*** showing a potential mechanism how DIO downregulates Wnt signaling pathway and regulate cell proliferation in colon. First, DIO suppresses Wnt signaling activators - *Wnt2, Wnt7b* and *Wnt5a* while upregulates Wnt antagonist - *Sfrp2* and *Sfrp5* expression, which consequently impairs cytosolic *Axin1-APC* interaction in the destruction complex that mediates Wnt signaling transduction, thus, leads to downregulated β-catenin expression on both gene and protein level. This DIO-induced downregulation of β-catenin further triggers downregulated *cMyc*, *p21* and *Raf-1* expression, together they contribute to the upregulation of downstream *CyclinD1* expression, which is correlated to the expression of Ki-67, indicating an elevated cell proliferation activity in colon.

Although the detailed mechanism behind which diet-induced-obesity regulates cell proliferation through interactions among several signaling, including Wnt, remains unclear, findings of this current study still provides evidence for the connection between diet-induced-obesity and disrupted Wnt signaling, and proves that proliferative activity is influenced consequently. Therefore, it is crucial to take Wnt signaling as well as β-catenin expression and localization into consideration when examine patients during clinical trials, because it could be an indicator for colon health.

TABLE AND FIGURES

Table 1. mRNA Expression of Genes Involved in Several Pathways

Pathway Identification	Gene	Control	DIO	Fold Change in DIO	P-value
Non-canonical Wnt Signaling	WNT5a	8.59±2.66	3.04±0.50	-0.65	0.0367
Canonical Wnt Signaling	SFRP2	74.04±16.04	200.23±56.77	1.7	0.032
	SFRP5	2.59±0.40	7.38±2.41	1.85	0.0425
	APC	1.07±0.41	0.70±0.19	-0.35	0.2251
	WNT2	4.53±1.42	2.58±0.83	-0.43	0.1354
	WNT7b	23.56±5.79	11.02±3.67	-0.53	0.048
	AXIN1	2.58±0.81	0.99±0.29	-0.62	0.0492
	CTNNB1	0.88±0.29	0.29±0.06	-0.67	0.0428
Cell Cycle/Proliferation/Apoptosis	CYCLIN D1	13.80±3.98	42.67±10.05	2.09	0.0114
	C-MYC	4.10±1.36	1.49±0.39	-0.64	0.0499
	P21	14.92±5.53	3.91±0.80	-0.74	0.0429
	RAF1	0.07±0.03	0.01±0.003	-0.86	0.0348
Endocytic Pathways	AGAP2	2.71±0.87	2.82±0.56	0.04	0.4598
Cell Invasion	PKP2	0.57±0.26	0.78±0.18	0.37	0.2636

Table 1. mRNA expression of β-catenin and genes in other selected signaling pathways in the colon of male mice in either control or DIO group. Quantity results are presented as normalized ratio to reference genes in mean±SEM (n=12); An increased expression of specific gene in DIO leads to positive fold change while decreased expression leads to negative fold change; fold change is calculated by subtracting CON gene expression from DIO gene expression, then divided by CON gene expression; p-value indicates the significance on gene expression change in DIO comparing to control mice.

Figure 1

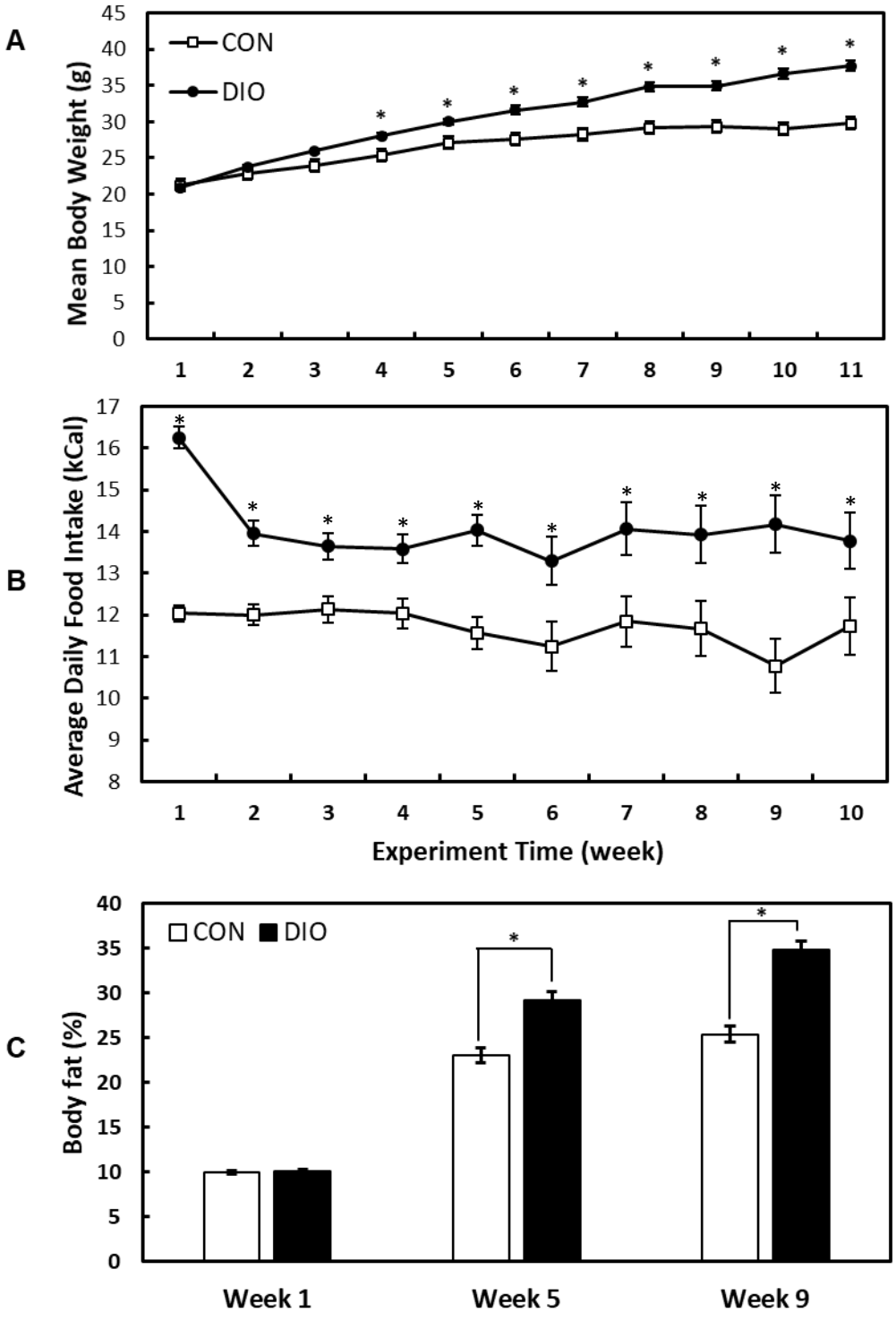

Figure 1. Average food intake (in kcal) and body composition change between control and DIO mice during experiment period.

Figure 1 (cont.)

A: Meaningful change of mean body weight between control and DIO group was observed starting from the 4th week of experiment, and the significance grew as experiment went on until the end of the trial;

B: Mean food intake per animal per day in kcal was significantly different at the first week of the experiment and remains different through the experimental period until the end of the trial;

C: The mean body fat percentage measured by MRI between control and DIO group was identical at the beginning of the experiment, however, after 4 weeks, a significant difference was observed, and the significance remains until the end of trial.

Figure 2

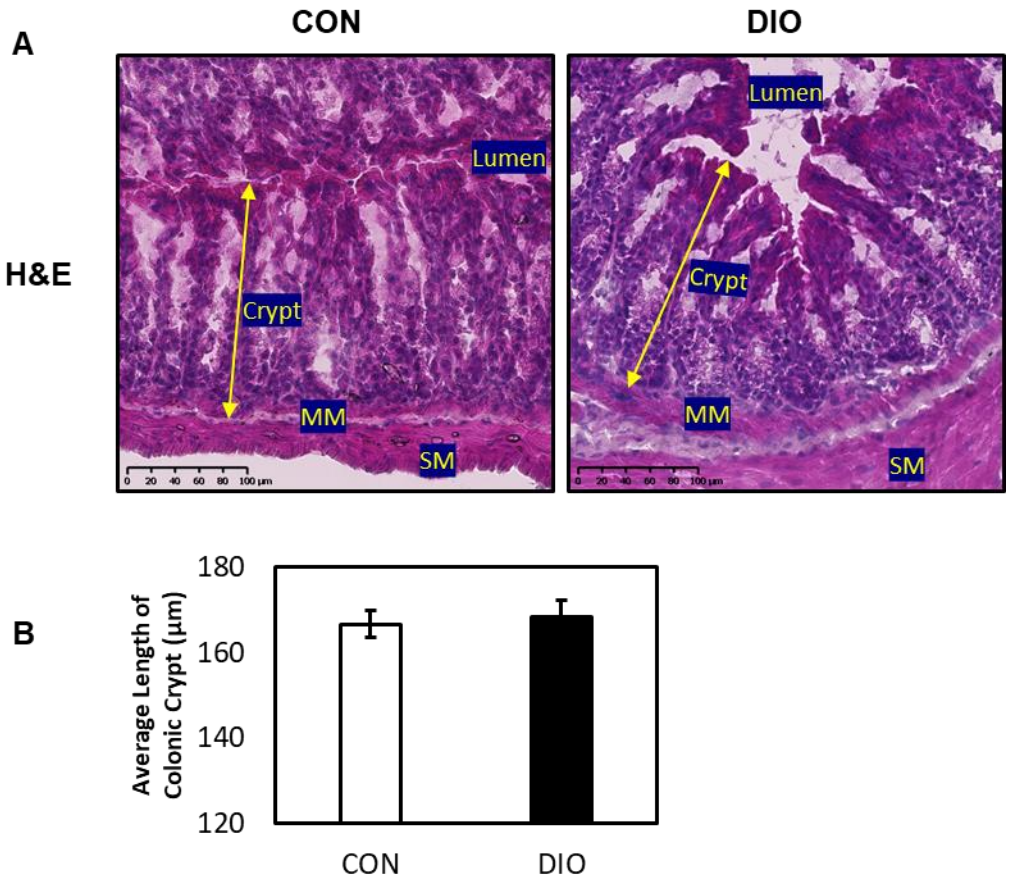

Figure 2. Histological analysis suggests no diet effect on colonic structure of mice between control and DIO group.

A: H&E straining was conducted in mice from both control and DIO group to conduct histological analysis and observe colonic crypt structures in detail. (***SM:*** Submucosa ***MM:*** Muscularis mucosae)

B: Independent t-test assuming equal variance was performed to analyze the mean crypt length of colon tissue from mice in control or DIO group (5 measurements per animal, n=12 per group). The results are presented in mean±SEM (μm). No significant difference was detected, suggesting that diet does not affect the basic structure in the colon of mice.

Figure 3

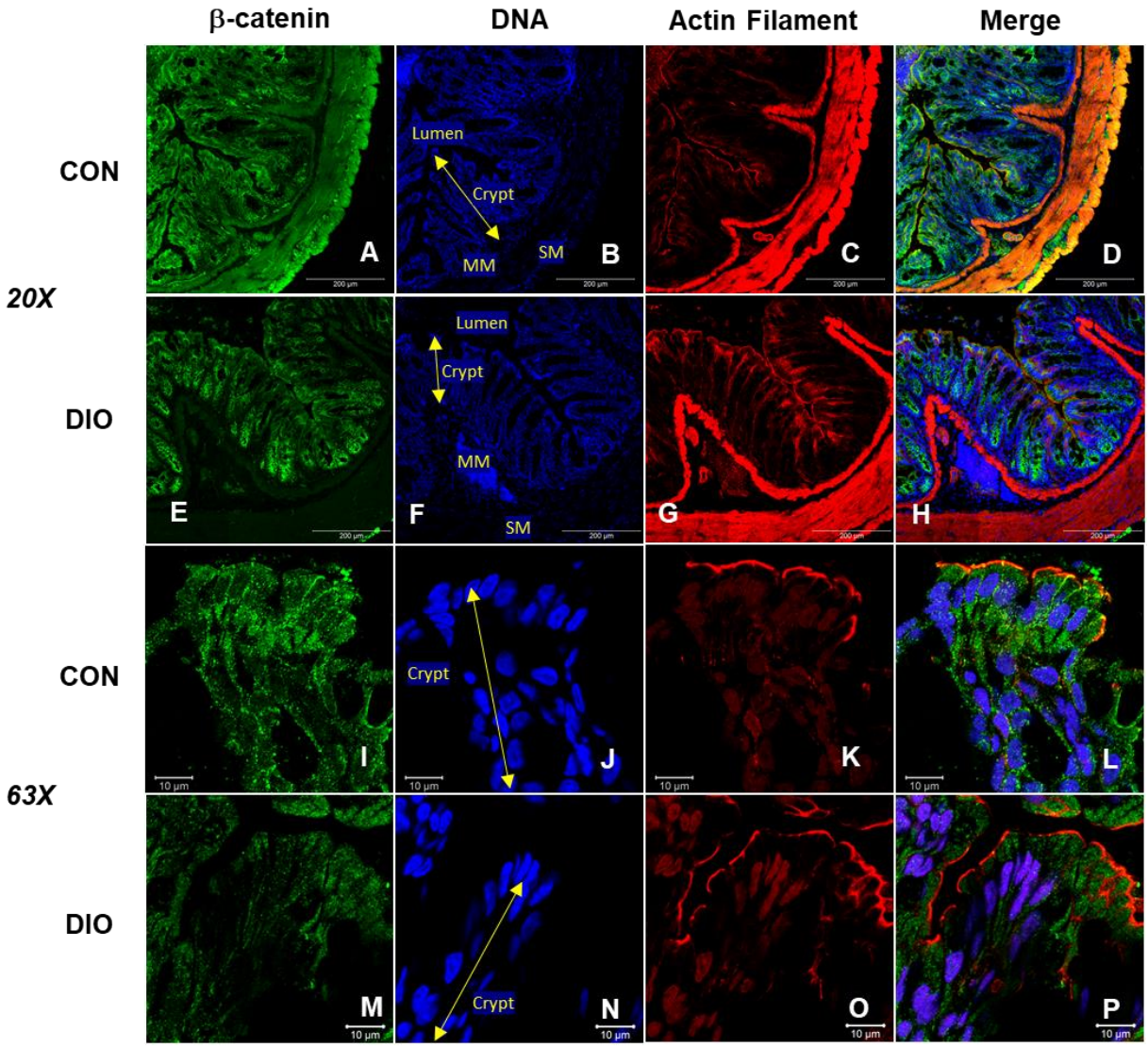
β-catenin
DNA
Actin Filament
Merge
CON
20X
DIO
CON
63X
DIO
Lumen
Crypt
MM
SM
A
B
C
D
E
F
G
H
I
J
K
L
M
N
O
P
10 μm
200 μm

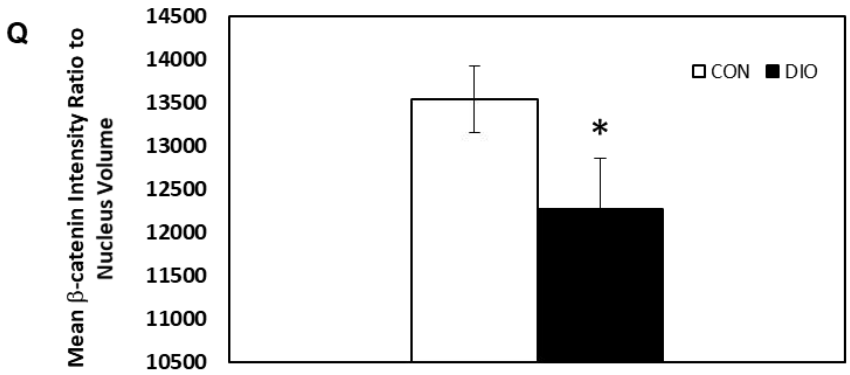
Q
Mean β-catenin Intensity Ratio to Nucleus Volume
14500
14000
13500
13000
12500
12000
11500
11000
10500
CON
DIO
*

Figure 3. Confocal immunofluorescent analysis of mouse colon using β-Catenin (green; A, E, I, M), actin filament (red; C, G, K, O), DRAQ5 pseudo-color that marks DNA (blue; B, F, J, N) and merged pictures (D, H, L, P) to visualize β-catenin accumulation and localization in 20X and 63X Oil magnification. (***SM:*** Submucosa ***MM:*** Muscularis mucosae)

A-H: Under 20X Oil magnification, intense green signal suggesting stronger β-Catenin accumulation on submucosa and at the simple columnar epithelium in colon tissue from CON and DIO mice;

I-P: Under 63X magnification, more intense green signal from β-Catenin accumulation was observed in colon tissue from DIO mice, especially at the bottom part of crypt near the submucosa, indicating the change of β-Catenin accumulation between CON and DIO mice happened not only on subcellular level but also on cellular level;

Q: Independent t-test assuming unequal variance was performed to analyze the relative level of β-Catenin nuclear accumulation in colon tissue from DIO and CON mice (22 measurements per group). The results are presented as β-Catenin immunofluorescence signal intensity ratio to nucleus volume (μm^3), in the form of Mean±SEM. Significant difference was detected, suggesting that diet has strong effect on the β-Catenin accumulation in the colon of mice.

Figure 4

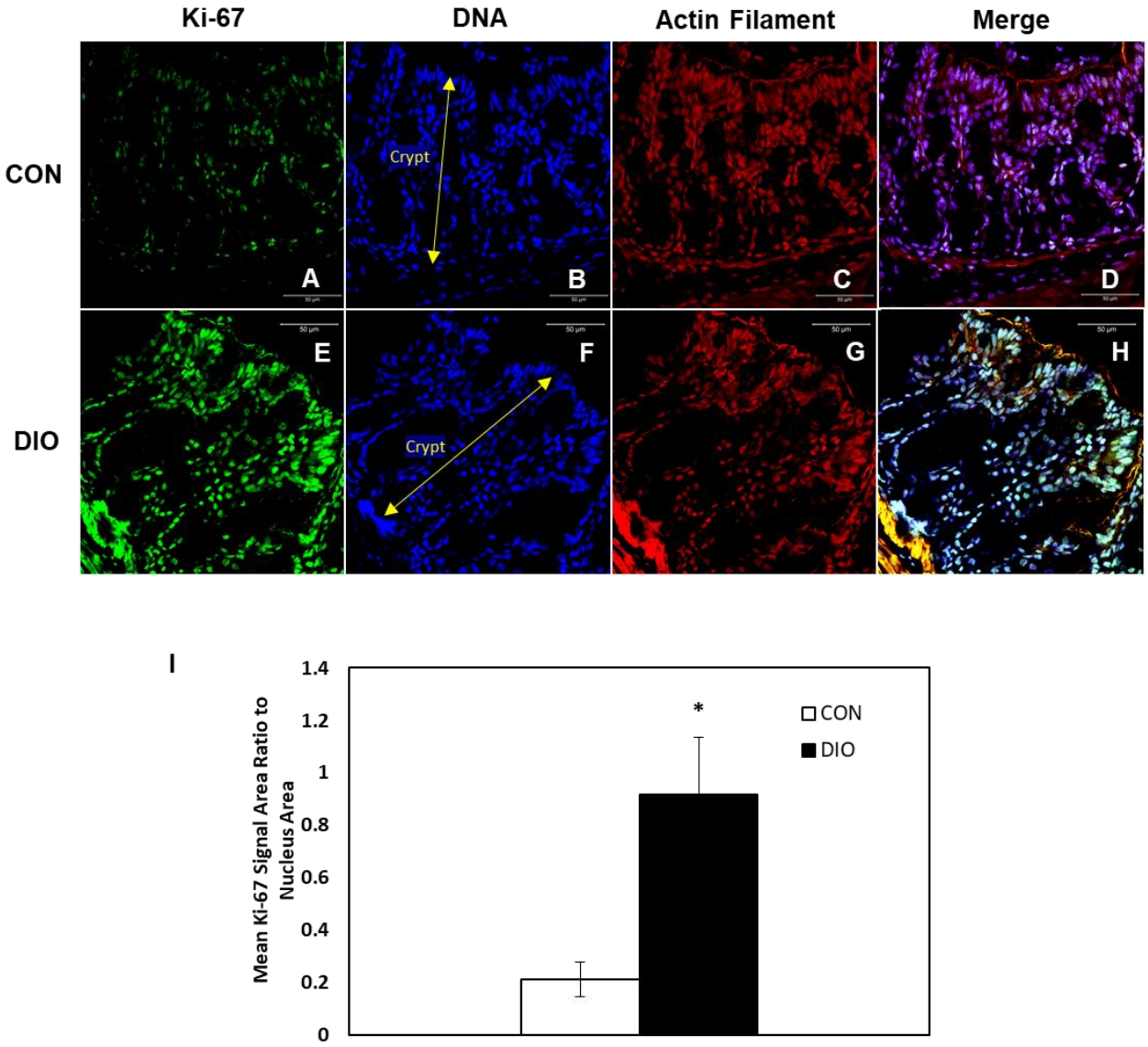

Figure 4. Confocal immunofluorescent analysis of mouse colon using Ki-67 (green; A and E), actin filament (red; C and G) and DRAQ5 pseudocolor that marks DNA (blue; B and F) and merged pictures (D and H) to visualize Ki-67 expression and localization in 20X magnification.

A-D: weak green signal suggesting low Ki-67 expression on both submucosa and on the crypt in colon tissue from CON mice;

Figure 4 (cont.)

E-H: intense green signal suggesting high Ki-67 expression on both submucosa and along the crypt in colon tissue from DIO mice;

I: Independent t-test assuming unequal variance was performed to analyze the relative level of Ki-67 expression in colon tissue from DIO and CON mice (5 measurements per group). The results are presented as Ki-67 immunofluorescence signal area (μm^3) ratio to nucleus signal area (μm^3), in the form of Mean±SEM. Significant difference was detected, suggesting that diet has strong effect on the Ki-67 expression in the colon of mice.

Figure 5

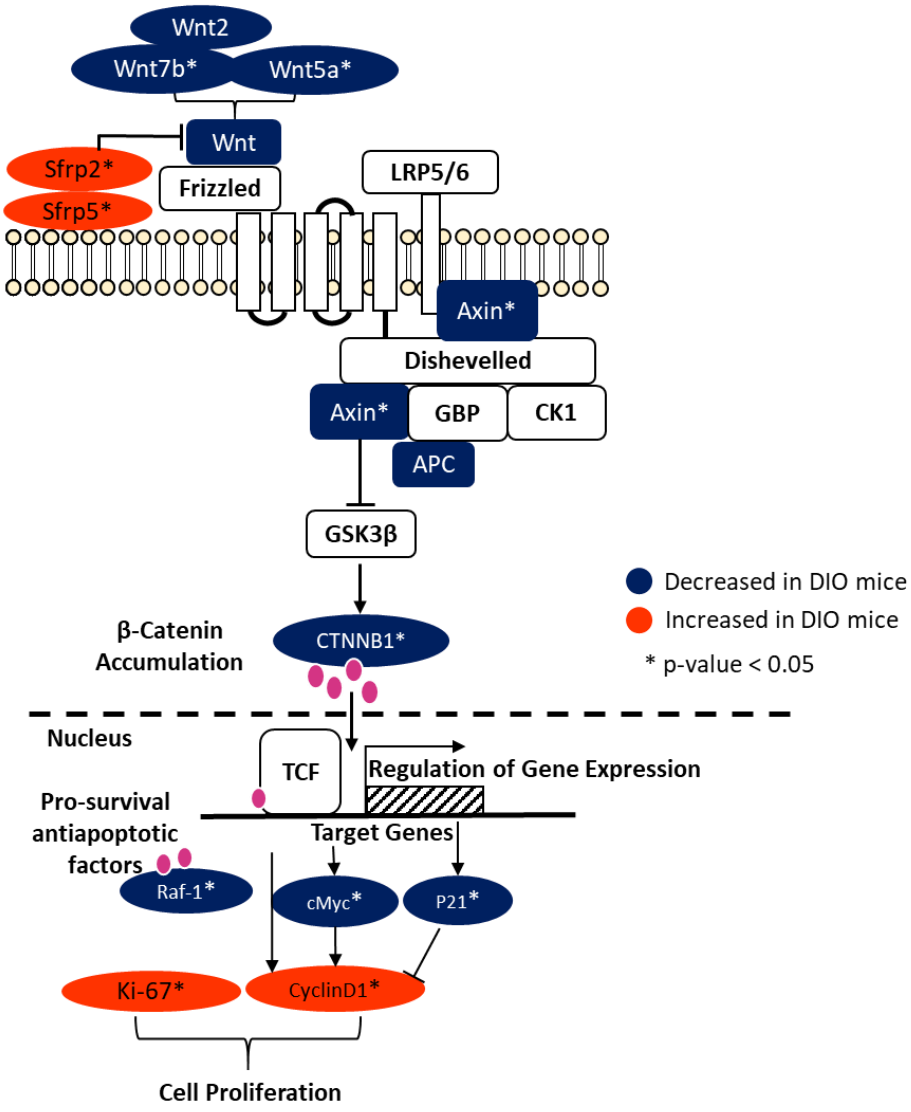

Figure 5. Schematic of genes examined in the current study that involved in the potential mechanisms through which DIO suppresses β-catenin, regulating Wnt signaling and cell cycle in colon of DIO mice.

REFERENCES

1. Bassett MT, Perl S. Obesity: the public health challenge of our time. Am J Public Health 2004;94(9):1477.
2. Cheong Y, Sadek KH, Bruce KD, Macklon N, Cagampang FR. Diet-induced maternal obesity alters ovarian morphology and gene expression in the adult mouse offspring. Fertil Steril 2014;102(3):899-907. doi: 10.1016/j.fertnstert.2014.06.015.
3. Peng Y, Rideout D, Rakita S, Lee J, Murr M. Diet-induced obesity associated with steatosis, oxidative stress, and inflammation in liver. Surg Obes Relat Dis 2012;8(1):73-81. doi: 10.1016/j.soard.2011.07.019.
4. de Git KC, Adan RA. Leptin resistance in diet-induced obesity: the role of hypothalamic inflammation. Obes Rev 2015;16(3):207-24. doi: 10.1111/obr.12243.
5. Dhahri W, Drolet MC, Roussel E, Couet J, Arsenault M. Chronic high-fat diet-induced obesity decreased survival and increased hypertrophy of rats with experimental eccentric hypertrophy from chronic aortic regurgitation. BMC Cardiovasc Disord 2014;14:123. doi: 10.1186/1471-2261-14-123.
6. Cui XR, Long CL, Tian J, Zhu J. Protective Effects of Fluvastatin on Reproductive Function in Obese Male Rats Induced by High-Fat Diet through Enhanced Signaling of mTOR. Cell Physiol Biochem 2017;41(2):598-608. doi: 10.1159/000457881.
7. Hart-Unger S, Arao Y, Hamilton KJ, Lierz SL, Malarkey DE, Hewitt SC, Freemark M, Korach KS. Hormone signaling and fatty liver in females: analysis of estrogen receptor alpha mutant mice. Int J Obes (Lond) 2017. doi: 10.1038/ijo.2017.50.
8. Yang R, Barouch LA. Leptin signaling and obesity: cardiovascular consequences. Circ Res 2007;101(6):545-59. doi: 10.1161/CIRCRESAHA.107.156596.
9. Zhu MJ, Du M, Nathanielsz PW, Ford SP. Maternal obesity up-regulates inflammatory signaling pathways and enhances cytokine expression in the mid-gestation sheep placenta. Placenta 2010;31(5):387-91. doi: 10.1016/j.placenta.2010.02.002.
10. Fei W, Tian DR, Tso P, Han JS. Diet-induced obese rats exhibit impaired LKB1-AMPK signaling in hypothalamus and adipose tissue. Peptides 2012;35(1):23-30. doi: 10.1016/j.peptides.2012.02.003.
11. Zhao X, Xiaoli, Zong H, Abdulla A, Yang ES, Wang Q, Ji JY, Pessin JE, Das BC, Yang F. Inhibition of SREBP transcriptional activity by a boron-containing compound improves lipid homeostasis in diet-induced obesity. Diabetes 2014;63(7):2464-73. doi: 10.2337/db13-0835.
12. Holstein TW. The evolution of the Wnt pathway. Cold Spring Harb Perspect Biol 2012;4(7):a007922. doi: 10.1101/cshperspect.a007922.
13. Clevers H, Nusse R. Wnt/beta-catenin signaling and disease. Cell 2012;149(6):1192-205. doi: 10.1016/j.cell.2012.05.012.
14. Kahn M. Can we safely target the WNT pathway? Nat Rev Drug Discov 2014;13(7):513-32. doi: 10.1038/nrd4233.
15. George SJ. Wnt pathway: a new role in regulation of inflammation. Arterioscler Thromb Vasc Biol 2008;28(3):400-2. doi: 10.1161/ATVBAHA.107.160952.
16. Schaale K, Neumann J, Schneider D, Ehlers S, Reiling N. Wnt signaling in macrophages: augmenting and inhibiting mycobacteria-induced inflammatory responses. Eur J Cell Biol 2011;90(6-7):553-9. doi: 10.1016/j.ejcb.2010.11.004.
17. Ma B, Hottiger MO. Crosstalk between Wnt/beta-Catenin and NF-kappaB Signaling Pathway during Inflammation. Front Immunol 2016;7:378. doi: 10.3389/fimmu.2016.00378.
18. Niehrs C. The complex world of WNT receptor signalling. Nat Rev Mol Cell Biol 2012;13(12):767-79. doi: 10.1038/nrm3470.

19. Lustig B, Jerchow B, Sachs M, Weiler S, Pietsch T, Karsten U, van de Wetering M, Clevers H, Schlag PM, Birchmeier W, et al. Negative feedback loop of Wnt signaling through upregulation of conductin/axin2 in colorectal and liver tumors. Mol Cell Biol 2002;22(4):1184-93.
20. Lien WH, Fuchs E. Wnt some lose some: transcriptional governance of stem cells by Wnt/beta-catenin signaling. Genes Dev 2014;28(14):1517-32. doi: 10.1101/gad.244772.114.
21. Birdsey GM, Shah AV, Dufton N, Reynolds LE, Osuna Almagro L, Yang Y, Aspalter IM, Khan ST, Mason JC, Dejana E, et al. The endothelial transcription factor ERG promotes vascular stability and growth through Wnt/beta-catenin signaling. Dev Cell 2015;32(1):82-96. doi: 10.1016/j.devcel.2014.11.016.
22. Zhang KS, Zhou Q, Wang YF, Liang LJ. Inhibition of Wnt signaling induces cell apoptosis and suppresses cell proliferation in cholangiocarcinoma cells. Oncol Rep 2013;30(3):1430-8. doi: 10.3892/or.2013.2560.
23. Stefater JA, 3rd, Lewkowich I, Rao S, Mariggi G, Carpenter AC, Burr AR, Fan J, Ajima R, Molkentin JD, Williams BO, et al. Regulation of angiogenesis by a non-canonical Wnt-Flt1 pathway in myeloid cells. Nature 2011;474(7352):511-5. doi: 10.1038/nature10085.
24. Povinelli BJ, Nemeth MJ. Wnt5a regulates hematopoietic stem cell proliferation and repopulation through the Ryk receptor. Stem Cells 2014;32(1):105-15. doi: 10.1002/stem.1513.
25. Famili F, Perez LG, Naber BA, Noordermeer JN, Fradkin LG, Staal FJ. The non-canonical Wnt receptor Ryk regulates hematopoietic stem cell repopulation in part by controlling proliferation and apoptosis. Cell Death Dis 2016;7(11):e2479. doi: 10.1038/cddis.2016.380.
26. Cancer Genome Atlas N. Comprehensive molecular characterization of human colon and rectal cancer. Nature 2012;487(7407):330-7. doi: 10.1038/nature11252.
27. Reya T, Clevers H. Wnt signalling in stem cells and cancer. Nature 2005;434(7035):843-50. doi: 10.1038/nature03319.
28. Yang AD, Fan F, Camp ER, van Buren G, Liu W, Somcio R, Gray MJ, Cheng H, Hoff PM, Ellis LM. Chronic oxaliplatin resistance induces epithelial-to-mesenchymal transition in colorectal cancer cell lines. Clin Cancer Res 2006;12(14 Pt 1):4147-53. doi: 10.1158/1078-0432.CCR-06-0038.
29. Sebio A, Kahn M, Lenz HJ. The potential of targeting Wnt/beta-catenin in colon cancer. Expert Opin Ther Targets 2014;18(6):611-5. doi: 10.1517/14728222.2014.906580.
30. Beier EE, Inzana JA, Sheu TJ, Shu L, Puzas JE, Mooney RA. Effects of Combined Exposure to Lead and High-Fat Diet on Bone Quality in Juvenile Male Mice. Environ Health Perspect 2015;123(10):935-43. doi: 10.1289/ehp.1408581.
31. Chen JR, Lazarenko OP, Wu X, Tong Y, Blackburn ML, Shankar K, Badger TM, Ronis MJ. Obesity reduces bone density associated with activation of PPARgamma and suppression of Wnt/beta-catenin in rapidly growing male rats. PLoS One 2010;5(10):e13704. doi: 10.1371/journal.pone.0013704.
32. Lu XM, Zhao H, Wang EH. A high-fat diet induces obesity and impairs bone acquisition in young male mice. Mol Med Rep 2013;7(4):1203-8. doi: 10.3892/mmr.2013.1297.
33. Frey JL, Li Z, Ellis JM, Zhang Q, Farber CR, Aja S, Wolfgang MJ, Clemens TL, Riddle RC. Wnt-Lrp5 signaling regulates fatty acid metabolism in the osteoblast. Mol Cell Biol 2015;35(11):1979-91. doi: 10.1128/MCB.01343-14.
34. Davis JE, Cain J, Banz WJ, Peterson RG. Age-Related Differences in Response to High-Fat Feeding on Adipose Tissue and Metabolic Profile in ZDSD Rats. ISRN Obes 2013;2013:584547. doi: 10.1155/2013/584547.
35. Tang Q, Chen C, Zhang Y, Dai M, Jiang Y, Wang H, Yu M, Jing W, Tian W. Wnt5a regulates the cell proliferation and adipogenesis via MAPK-independent pathway in early stage of obesity. Cell Biol Int 2018;42(1):63-74. doi: 10.1002/cbin.10862.

36. Chen ZL, Shao WJ, Xu F, Liu L, Lin BS, Wei XH, Song ZL, Lu HG, Fantus IG, Weng JP, et al. Acute Wnt pathway activation positively regulates leptin gene expression in mature adipocytes. Cell Signal 2015;27(3):587-97. doi: 10.1016/j.cellsig.2014.12.012.
37. Chen X, Iriscilla A, Shannon C, Fourcaudot M, Acharya NK, Jenkinson CP, Heikkinen S, Norton L. The Diabetes Gene and Wnt Pathway Effector TCF7L2 Regulates Adipocyte Development and Function. Diabetes 2018. doi: 10.2337/db17-0318.
38. Zhou D, Lezmi S, Wang H, Davis J, Banz W, Chen H. Fat accumulation in the liver of obese rats is alleviated by soy protein isolate through beta-catenin signaling. Obesity (Silver Spring) 2014;22(1):151-8. doi: 10.1002/oby.20421.
39. Behari J, Li H, Liu S, Stefanovic-Racic M, Alonso L, O'Donnell CP, Shiva S, Singamsetty S, Watanabe Y, Singh VP, et al. beta-catenin links hepatic metabolic zonation with lipid metabolism and diet-induced obesity in mice. Am J Pathol 2014;184(12):3284-98. doi: 10.1016/j.ajpath.2014.08.022.
40. Zhai X, Yan K, Fan J, Niu M, Zhou Q, Zhou Y, Chen H, Zhou Y. The beta-catenin pathway contributes to the effects of leptin on SREBP-1c expression in rat hepatic stellate cells and liver fibrosis. Br J Pharmacol 2013;169(1):197-212. doi: 10.1111/bph.12114.
41. Benzler J, Andrews ZB, Pracht C, Stohr S, Shepherd PR, Grattan DR, Tups A. Hypothalamic WNT signalling is impaired during obesity and reinstated by leptin treatment in male mice. Endocrinology 2013;154(12):4737-45. doi: 10.1210/en.2013-1746.
42. Elghazi L, Gould AP, Weiss AJ, Barker DJ, Callaghan J, Opland D, Myers M, Cras-Meneur C, Bernal-Mizrachi E. Importance of beta-Catenin in glucose and energy homeostasis. Sci Rep 2012;2:693. doi: 10.1038/srep00693.
43. Gai Z, Hiller C, Chin SH, Hofstetter L, Stieger B, Konrad D, Kullak-Ublick GA. Uninephrectomy augments the effects of high fat diet induced obesity on gene expression in mouse kidney. Biochim Biophys Acta 2014;1842(9):1870-8. doi: 10.1016/j.bbadis.2014.07.001.
44. Strakovsky RS, Pan YX. A decrease in DKK1, a WNT inhibitor, contributes to placental lipid accumulation in an obesity-prone rat model. Biol Reprod 2012;86(3):81. doi: 10.1095/biolreprod.111.094482.
45. Delage B, Bairras C, Buaud B, Pallet V, Cassand P. A high-fat diet generates alterations in nuclear receptor expression: prevention by vitamin A and links with cyclooxygenase-2 and beta-catenin. Int J Cancer 2005;116(6):839-46. doi: 10.1002/ijc.21108.
46. Calle EE, Rodriguez C, Walker-Thurmond K, Thun MJ. Overweight, obesity, and mortality from cancer in a prospectively studied cohort of U.S. adults. N Engl J Med 2003;348(17):1625-38. doi: 10.1056/NEJMoa021423.
47. Penrose HM, Heller S, Cable C, Nakhoul H, Baddoo M, Flemington E, Crawford SE, Savkovic SD. High-fat diet induced leptin and Wnt expression: RNA-sequencing and pathway analysis of mouse colonic tissue and tumors. Carcinogenesis 2017;38(3):302-11. doi: 10.1093/carcin/bgx001.
48. Zhu QC, Gao RY, Wu W, Guo BM, Peng JY, Qin HL. Effect of a high-fat diet in development of colonic adenoma in an animal model. World J Gastroenterol 2014;20(25):8119-29. doi: 10.3748/wjg.v20.i25.8119.
49. Deng J, Miller SA, Wang HY, Xia W, Wen Y, Zhou BP, Li Y, Lin SY, Hung MC. beta-catenin interacts with and inhibits NF-kappa B in human colon and breast cancer. Cancer Cell 2002;2(4):323-34.
50. Daruwalla J, Nikfarjam M, Malcontenti-Wilson C, Muralidharan V, Christophi C. Effect of thalidomide on colorectal cancer liver metastases in CBA mice. J Surg Oncol 2005;91(2):134-40. doi: 10.1002/jso.20289.
51. Connelly DM, Taberner PV. Characterization of the spontaneous diabetes obesity syndrome in mature male CBA/Ca mice. Pharmacol Biochem Behav 1989;34(2):255-9.

52. al Qatari M, Shih MF, Taberner PV. Chronic ethanol consumption ameliorates the maturity-onset diabetes-obesity syndrome in CBA mice. Alcohol Alcohol 1996;31(1):89-99.
53. Vasilyeva ON, Frisina ST, Zhu X, Walton JP, Frisina RD. Interactions of hearing loss and diabetes mellitus in the middle age CBA/CaJ mouse model of presbycusis. Hear Res 2009;249(1-2):44-53. doi: 10.1016/j.heares.2009.01.007.
54. Holly VL, Widen SA, Famulski JK, Waskiewicz AJ. Sfrp1a and Sfrp5 function as positive regulators of Wnt and BMP signaling during early retinal development. Dev Biol 2014;388(2):192-204. doi: 10.1016/j.ydbio.2014.01.012.
55. Jaikanth C, Gurumurthy P, Indhumathi T, Cherian KM. Emergence of sfrp5 as a pleiotropic adipocytokine and its association with wnt signaling. Minerva Endocrinol 2014.
56. Su HY, Lai HC, Lin YW, Liu CY, Chen CK, Chou YC, Lin SP, Lin WC, Lee HY, Yu MH. Epigenetic silencing of SFRP5 is related to malignant phenotype and chemoresistance of ovarian cancer through Wnt signaling pathway. Int J Cancer 2010;127(3):555-67. doi: 10.1002/ijc.25083.
57. Schmeckpeper J, Verma A, Yin L, Beigi F, Zhang L, Payne A, Zhang Z, Pratt RE, Dzau VJ, Mirotsou M. Inhibition of Wnt6 by Sfrp2 regulates adult cardiac progenitor cell differentiation by differential modulation of Wnt pathways. J Mol Cell Cardiol 2015;85:215-25. doi: 10.1016/j.yjmcc.2015.06.003.
58. Sugiyama Y, Shelley EJ, Wen L, Stump RJ, Shimono A, Lovicu FJ, McAvoy JW. Sfrp1 and Sfrp2 are not involved in Wnt/beta-catenin signal silencing during lens induction but are required for maintenance of Wnt/beta-catenin signaling in lens epithelial cells. Dev Biol 2013;384(2):181-93. doi: 10.1016/j.ydbio.2013.10.008.
59. Brinkmann EM, Mattes B, Kumar R, Hagemann AI, Gradl D, Scholpp S, Steinbeisser H, Kaufmann LT, Ozbek S. Secreted Frizzled-related Protein 2 (sFRP2) Redirects Non-canonical Wnt Signaling from Fz7 to Ror2 during Vertebrate Gastrulation. J Biol Chem 2016;291(26):13730-42. doi: 10.1074/jbc.M116.733766.
60. Ouchi N, Higuchi A, Ohashi K, Oshima Y, Gokce N, Shibata R, Akasaki Y, Shimono A, Walsh K. Sfrp5 is an anti-inflammatory adipokine that modulates metabolic dysfunction in obesity. Science 2010;329(5990):454-7. doi: 10.1126/science.1188280.
61. Xiao X, Xiao Y, Wen R, Zhang Y, Li X, Wang H, Huang J, Liu J, Long T, Tang J. Promoting roles of the secreted frizzled-related protein 2 as a Wnt agonist in lung cancer cells. Oncol Rep 2015;34(5):2259-66. doi: 10.3892/or.2015.4221.
62. Chung MT, Lai HC, Sytwu HK, Yan MD, Shih YL, Chang CC, Yu MH, Liu HS, Chu DW, Lin YW. SFRP1 and SFRP2 suppress the transformation and invasion abilities of cervical cancer cells through Wnt signal pathway. Gynecol Oncol 2009;112(3):646-53. doi: 10.1016/j.ygyno.2008.10.026.
63. Mori H, Prestwich TC, Reid MA, Longo KA, Gerin I, Cawthorn WP, Susulic VS, Krishnan V, Greenfield A, Macdougald OA. Secreted frizzled-related protein 5 suppresses adipocyte mitochondrial metabolism through WNT inhibition. J Clin Invest 2012;122(7):2405-16. doi: 10.1172/JCI63604.
64. Wong SC, Lo ES, Lee KC, Chan JK, Hsiao WL. Prognostic and diagnostic significance of beta-catenin nuclear immunostaining in colorectal cancer. Clin Cancer Res 2004;10(4):1401-8.
65. Wong SC, Lo ES, Chan AK, Lee KC, Hsiao WL. Nuclear beta catenin as a potential prognostic and diagnostic marker in patients with colorectal cancer from Hong Kong. Mol Pathol 2003;56(6):347-52.
66. Hugh TJ, Dillon SA, Taylor BA, Pignatelli M, Poston GJ, Kinsella AR. Cadherin-catenin expression in primary colorectal cancer: a survival analysis. Br J Cancer 1999;80(7):1046-51. doi: 10.1038/sj.bjc.6690461.

67. Cheah PY, Choo PH, Yao J, Eu KW, Seow-Choen F. A survival-stratification model of human colorectal carcinomas with beta-catenin and p27kip1. Cancer 2002;95(12):2479-86. doi: 10.1002/cncr.10986.
68. Nazemalhosseini Mojarad E, Kashfi SM, Mirtalebi H, Almasi S, Chaleshi V, Kishani Farahani R, Tarban P, Molaei M, Zali MR, P JKK. Prognostic Significance of Nuclear beta-Catenin Expression in Patients with Colorectal Cancer from Iran. Iran Red Crescent Med J 2015;17(7):e22324. doi: 10.5812/ircmj.22324v2.
69. Baldus SE, Monig SP, Huxel S, Landsberg S, Hanisch FG, Engelmann K, Schneider PM, Thiele J, Holscher AH, Dienes HP. MUC1 and nuclear beta-catenin are coexpressed at the invasion front of colorectal carcinomas and are both correlated with tumor prognosis. Clin Cancer Res 2004;10(8):2790-6.
70. Wang L, Cheng H, Liu Y, Wang L, Yu W, Zhang G, Chen B, Yu Z, Hu S. Prognostic value of nuclear beta-catenin overexpression at invasive front in colorectal cancer for synchronous liver metastasis. Ann Surg Oncol 2011;18(6):1553-9. doi: 10.1245/s10434-010-1519-9.
71. Zhang S, Wang Z, Shan J, Yu X, Li L, Lei R, Lin D, Guan S, Wang X. Nuclear expression and/or reduced membranous expression of beta-catenin correlate with poor prognosis in colorectal carcinoma: A meta-analysis. Medicine (Baltimore) 2016;95(49):e5546. doi: 10.1097/MD.0000000000005546.
72. Pancione M, Forte N, Fucci A, Sabatino L, Febbraro A, Di Blasi A, Daniele B, Parente D, Colantuoni V. Prognostic role of beta-catenin and p53 expression in the metastatic progression of sporadic colorectal cancer. Hum Pathol 2010;41(6):867-76. doi: 10.1016/j.humpath.2009.09.019.
73. Pancione M, Forte N, Sabatino L, Tomaselli E, Parente D, Febbraro A, Colantuoni V. Reduced beta-catenin and peroxisome proliferator-activated receptor-gamma expression levels are associated with colorectal cancer metastatic progression: correlation with tumor-associated macrophages, cyclooxygenase 2, and patient outcome. Hum Pathol 2009;40(5):714-25. doi: 10.1016/j.humpath.2008.08.019.
74. Aaltomaa S, Karja V, Lipponen P, Isotalo T, Kankkunen JP, Talja M, Mokka R. Expression of Ki-67, cyclin D1 and apoptosis markers correlated with survival in prostate cancer patients treated by radical prostatectomy. Anticancer Res 2006;26(6C):4873-8.
75. Shevra CR, Ghosh A, Kumar M. Cyclin D1 and Ki-67 expression in normal, hyperplastic and neoplastic endometrium. J Postgrad Med 2015;61(1):15-20. doi: 10.4103/0022-3859.147025.
76. Lebe B, Pabuccuoglu U, Ozer E. The significance of Ki-67 proliferative index and cyclin D1 expression of dysplastic nevi in the biologic spectrum of melanocytic lesions. Appl Immunohistochem Mol Morphol 2007;15(2):160-4. doi: 10.1097/01.pai.0000209868.58699.64.
77. Kouraklis G, Theocharis S, Vamvakas P, Vagianos C, Glinavou A, Giaginis C, Sioka C. Cyclin D1 and Rb protein expression and their correlation with prognosis in patients with colon cancer. World J Surg Oncol 2006;4:5. doi: 10.1186/1477-7819-4-5.
78. Carlos de Vicente J, Herrero-Zapatero A, Fresno MF, Lopez-Arranz JS. Expression of cyclin D1 and Ki-67 in squamous cell carcinoma of the oral cavity: clinicopathological and prognostic significance. Oral Oncol 2002;38(3):301-8.
79. Meyer N, Penn LZ. Reflecting on 25 years with MYC. Nat Rev Cancer 2008;8(12):976-90. doi: 10.1038/nrc2231.
80. Bretones G, Delgado MD, Leon J. Myc and cell cycle control. Biochim Biophys Acta 2015;1849(5):506-16. doi: 10.1016/j.bbagrm.2014.03.013.
81. Zhang DY, Wang HJ, Tan YZ. Wnt/beta-catenin signaling induces the aging of mesenchymal stem cells through the DNA damage response and the p53/p21 pathway. PLoS One 2011;6(6):e21397. doi: 10.1371/journal.pone.0021397.

82. Chen A, Huang X, Xue Z, Cao D, Huang K, Chen J, Pan Y, Gao Y. The Role of p21 in Apoptosis, Proliferation, Cell Cycle Arrest, and Antioxidant Activity in UVB-Irradiated Human HaCaT Keratinocytes. Med Sci Monit Basic Res 2015;21:86-95. doi: 10.12659/MSMBR.893608.
83. Leicht DT, Balan V, Kaplun A, Singh-Gupta V, Kaplun L, Dobson M, Tzivion G. Raf kinases: function, regulation and role in human cancer. Biochim Biophys Acta 2007;1773(8):1196-212. doi: 10.1016/j.bbamcr.2007.05.001.
84. Chang CJ, Yang JY, Xia W, Chen CT, Xie X, Chao CH, Woodward WA, Hsu JM, Hortobagyi GN, Hung MC. EZH2 promotes expansion of breast tumor initiating cells through activation of RAF1-beta-catenin signaling. Cancer Cell 2011;19(1):86-100. doi: 10.1016/j.ccr.2010.10.035.
85. Jeon SH, Yoon JY, Park YN, Jeong WJ, Kim S, Jho EH, Surh YJ, Choi KY. Axin inhibits extracellular signal-regulated kinase pathway by Ras degradation via beta-catenin. J Biol Chem 2007;282(19):14482-92. doi: 10.1074/jbc.M611129200.
86. Park KS, Jeon SH, Kim SE, Bahk YY, Holmen SL, Williams BO, Chung KC, Surh YJ, Choi KY. APC inhibits ERK pathway activation and cellular proliferation induced by RAS. J Cell Sci 2006;119(Pt 5):819-27. doi: 10.1242/jcs.02779.
87. Gougelet A, Colnot S. A Complex Interplay between Wnt/beta-Catenin Signalling and the Cell Cycle in the Adult Liver. Int J Hepatol 2012;2012:816125. doi: 10.1155/2012/816125.
88. Zhang J, Gill AJ, Issacs JD, Atmore B, Johns A, Delbridge LW, Lai R, McMullen TP. The Wnt/beta-catenin pathway drives increased cyclin D1 levels in lymph node metastasis in papillary thyroid cancer. Hum Pathol 2012;43(7):1044-50. doi: 10.1016/j.humpath.2011.08.013.
89. Pasz-Walczak G, Kordek R, Faflik M. P21 (WAF1) expression in colorectal cancer: correlation with P53 and cyclin D1 expression, clinicopathological parameters and prognosis. Pathol Res Pract 2001;197(10):683-9. doi: 10.1078/0344-0338-00146.
90. Kim WG, Park JW, Willingham MC, Cheng SY. Diet-induced obesity increases tumor growth and promotes anaplastic change in thyroid cancer in a mouse model. Endocrinology 2013;154(8):2936-47. doi: 10.1210/en.2013-1128.
91. Park SY, Kim JS, Seo YR, Sung MK. Effects of diet-induced obesity on colitis-associated colon tumor formation in A/J mice. Int J Obes (Lond) 2012;36(2):273-80. doi: 10.1038/ijo.2011.83.

APPENDIX A
SUPPLEMENTARY TABLES

Supplementary Table 1. Diet Formula

Diet Formula	***Control***		***High Fat***	
	gm%	kcal%	gm%	kcal%
Protein	19.2	20	24	20
Carbohydrate	67.3	70	41	35
Fat	4.3	10	24	45
Total		100		100
kcal/gm	3.85		4.73	
	gm	kcal	gm	kcal
Casein, 30 Mesh	200	800	200	800
L-Cystine	3	12	3	12
Corn Starch	452.2	1808.8	72.8	291
Maltodextrin 10	75	300	100	400
Sucrose	172.8	691.2	172.8	691
Cellulose, BW200	50	0	50	0
Soybean Oil	25	225	25	225
Lard	20	180	177.5	1598
Mineral Mix S10026	10	0	10	0
DiCalcium Phosphate	13	0	13	0
Calcium Carbonate	5.5	0	5.5	0
Potassium Citrate, 1 H2O	16.5	0	16.5	0
Vitamin Mix V10001	10	40	10	40
Choline Bitartrate	2	0	2	0
FD&C Yellow Dye#5	0.04	0	N/A	N/A
FD&C Red Dye#40	0.01	0	0.05	0
Total	1055.05	4057	858.15	4057

*The diet formula is provided by http://www.researchdiets.com/

Supplementary Table 2. List of Primers

Gene Name	Ensembl Transcription ID	Position	Sequence	Amplification Efficiency*
mL7a	ENSMUST000001028986	Forward +176	5'-AACTTCGGCATTGGACAGGACA-3'	100.521%
		Reverse +289	5'-TTTGAGCCGCTTGTAGAGGATAGC-3'	
mActB	ENSMUST00000102507.9	Forward +153	5'-GAT GCT CCC CGG GCT GTA TT-3'	107.079%
		Reverse +219	5'-TTC CCA CCA TCA CAC CCT GG-3'	
mGADPH	ENSMUSE00001143324	Forward +65	5'-TTG ATG AGT ATG AAG TGC CC-3'	98.744%
		Reverse +153	5'-GCT GGA GTA GCC ATT CTA AT-3'	
mP21	ENSMUST00000023829	Forward +32	5'-CAGAGTCTAGGGGAATTGGAGTCAG-3'	104.066%
		Reverse +97	5'-CCTGTGGCTCTGAATGTCTGGA-3'	
mWnt5a	ENSMUST00000112272	Forward +555	5'-GCTGCGGAGACAACATCGACTATG-3'	100.741%
		Reverse +621	5'-TCCCTTTCTCTAGCGTCCACGAAC-3'	
mc-Myc	ENSMUST00000188482	Forward +1369	5'-CCAGCAGCGACTCTGAAGAAGAGC-3'	102.196%
		Reverse +1459	5'-TCCGACCTCTTGGCAGGGGTTT-3'	
mSfrp2	ENSMUST00000029625	Forward +491	5'-CACCAAGAAGTTCCTGTGCTCGC-3	92.928%
		Reverse +564	5'-GACACGGCTGGATGGTCTCATCT-3'	
mSfrp5	ENSMUST00000018966	Forward +807	5'-GCCTCATGGAACAGATGTG-3'	97.896%
		Reverse +884	5'-GGTCCCCGTTGTCTATCTT-3'	
mWnt2	ENSMUST00000010941	Forward +803	5'-CGTGCCTTTGTAGATGCCA-3'	98.379%
		Reverse +895	5'-CTTTACAGCCTTCCTTCCAGC-3'	
mCyclinD1	ENSMUST00000060455	Forward +254	5'-GAGCGTTACCAGAACCTGTCTCCA-3'	101.111%
		Reverse +319	5'-AAGTGCGTTGTCAGAACAGTGGCT-3'	
mWnt7b	ENSMUST00000023015	Forward +878	5'-CCGTGAGATCAAAAAGAACGCCAGG-3'	100.106%
		Reverse +945	5'-GAACCTTTCTGCCCGCCTCATTGTT-3'	
mRAF1	ENSMUST00000000451	Forward +1270	5'-CGAAGTCACAGTGAATCAGCCTCA-3'	96.041%
		Reverse +1333	5'-TTGGACTCAGGTTGTTTGGGCT-3'	
mCTNNB1	ENSMUST00000007130.14	Forward +980	5'-CTTTAAGTCTGGTGGCATCC-3'	93.86%
		Reverse +1058	5'-CGTGATGGCGTAGAACAGTA-3'	
mAxin 1	ENSMUST00000074370.9	Forward +1647F	5'-GGCTGAAGAAAAGTTGGAGGAACG-3'	92.726%
		Reverse+ 1715R	5'-ATTTCACCATCCTCCCCTTCTTCC-3'	
mAPC	ENSMUST00000079362.11	Forward +1171F	5'-CCAGTGTTTTGAGTTCTAGCGGCA-3'	96.51%
		Reverse +1239R	5'-CCTTTGTCCCCAGATGACTTGTCA-3'	

*The qPCR amplification efficiency is calculated based on the slope of the standard curve (https://www.lifetechnologies.com/us/en/home/brands/thermo-scientific/molecular-biology/molecular-biology-learning-center/molecular-biology-resource-library/thermo-scientific-web-tools/qpcr-efficiency-calculator.html). Slopes between -3.1 and -3.6 giving reaction efficiencies between 90 and 120% are typically acceptable.